Southern Journal of Engineering & Technology – Special Issue, Vol. 01, Issue 01, 2024

Moment Curvature and Ductility of FRP-Reinforced Concrete Beams having Different Types of Fibers

Mehar Ali[1], Attiq Ur Rehman[1], Sultan Arshid[1], Ali Raza[1], Muhammad Arshad[1], Bilal Masood[2], Muhammad Hassan[1]

[1]Department of Civil Engineering, University of Engineering and Technology Taxila, 47080, Pakistan.

[2]Department of Civil Engineering, Wah Engineering College, University of Wah, Wah Cantt, 47040, Pakistan.

Abstract. The study investigated various fiber-reinforced polymer (FRP) bars and the flexural behavior of hybrid beams constructed by placing concretes produced with different fibers into glass fiber-reinforced polymer (GFRP) box profiles. Hybrid beams were created by incorporating polypropylene, steel, and glass fiber concretes into the GFRP box profiles. Additionally, flexural tests were conducted using carbon, aramid, glass, basalt, and steel bars in the tensile zone for each beam type. The load-deflection and moment-curvature graphs of the hybrid beams were plotted, and their ductility and moment-curvature were calculated and compared. The performance of the FRP bars and fiber types was interpreted and analyzed. The results were evaluated under two categories: the effects of bar type and fiber type on hybrid beam behavior. GFRP hybrid specimens with GH class exhibited the highest ductility.

Keywords: Beams, FRP Reinforced Beams, Ductility, Moment Curvature.

Email address: meharaliali25@gmail.com,

1. Introduction

The creation and design of many building materials have addressed worries regarding subpar quality, notwithstanding certain restrictions. Although steel and concrete are essential building materials, the poor tensile strength of concrete and the high weight and corrosion susceptibility of steel present serious obstacles to environmental sustainability. Researchers have focused a lot of work on designing sustainable building materials in an effort to overcome these problems. Fiber-reinforced polymer (FRP) composites, for instance, are becoming more and more well-liked because of their high tensile strength, low weight, and resistance to corrosion. Furthermore, it has been demonstrated through testing that using FRP composites in combination with traditional building materials can effectively reinforce and strengthen a variety of structural elements (Raza et al., 2021a; 2021b; 2021c; 2021d; 2022a; 2022b). Furthermore, a wide range of literature has been devoted to fiber-reinforced concrete material. For instance, different works may be consulted to assess the suitability of fibers with varying proportions and their intended characteristics in concrete (Hiremath et al., 2018; Aslani et al., 2019). In contrast to the aforementioned studies, the current work aims to combine a few topics as reported previously. For example, a few investigations can be noted to assess the suitability of numerous fiber types on the structural characteristics of hybrid beams. Yet, none of the available studies aims to assess the impact of these fiber types on hybrid beams fabricated by employing various types of FRP reinforcing bars. Consequently, this study intends to assess the most suited FRP re-bar and fiber type to enhance the structural response of beam specimens. The external confinement of concrete using FRP materials significantly enhances the structural properties of concrete (Raza et al., 2021; Berradia et al., 2022; 2023; Setvati and Mustaffa, 2018; Raza et al., 2021; Raza et al., 2020; El-Ouni and Raza, 2021; Aslam

et al., 2021; Ahmad and Raza, 2020). In place of the reference specimens made of concrete with steel reinforcing bars, this study examines hybrid beam specimens made of four different kinds of FRP bars: carbon, glass, aramid, and basalt fibers. Additionally, when creating multivariate experimental classes, three distinct types of fiber - steel, glass, and polypropylene - were incorporated into the concrete. In order to establish the profiles of the GFRP test specimens, these fibers were inserted. These results led to the development and analysis of ductility and moment-curvature graphs.

2. Methodology

2.1. Materials

GFRP box profiles with a length of 500 mm and cross-sectional dimensions of 75 x 75 x 4 mm. Additionally, in the tensile area of the hybrid beam specimens, there were FRP ribbed reinforcing bars with a 10 mm diameter. The test characteristics of steel, GFRP profiles, and FRP bars are listed in Table 1.

The GFRP box profile used concrete with a compressive strength of 37 MPa. Moreover, 1% of steel, polypropylene, and glass fibers were added to the fiber-reinforced concrete examples in order to investigate the effects of different types of fibers on the specimens' flexure strength. The stress-strain curves of FRP bars are displayed in Figure 1.

2.2. Fabrication and Testing of specimens

Restate the Five different classes of reinforcing bars were included for GFRP box profiling in order to test the specimens. The types that were selected were carbon reinforced polymer (CFRP) bars, steel bars, GFRP and basalt fiber reinforced polymer (BFRP) bars, and aramid fiber reinforced polymer (AFRP) bars.

Furthermore, three different classes of fibers - glass, polypropylene, and steel - were used in the experimental design to assess the flexural behavior of beam specimens. Furthermore, the flexural response and fracture toughness of the beam specimens were observed through the analysis of their moment-curvature and ductility. Two hybrid beams from each beam class were constructed as part of the experimental design, and the final plots were made using the mean values of the data.

Hybrid beam specimens made with plain concrete were labeled with the prefix ‘RH,’ serving as the control model. Specimens with steel fiber concrete were labeled ‘SH,’ and those with glass fibers were labeled ‘GH.’ The bars used to reinforce the tensile region of the flexural components were designated as steel, GFRP, AFRP, CFRP, and BFRP. For example, beam specimens without bars were referred to as ‘WH,’ while specimens without GFRP bars and fiber profiles were termed ‘Plain Concrete.’ Beam specimens with polypropylene fibers, glass fibers, and steel fibers were labeled ‘PFRC,’ ‘GFRC,’ and ‘SFRC,’ respectively.

RH-steel bars examples were hybrid specimens with lean concrete and steel bars reinforcing the tensile areas. GH-GFRP examples were hybrid specimens with glass fiber concrete and GFRP bars in the tensile areas. "PH-WR" specimens were concrete samples that had polypropylene fibers but no bars. All bars - GFRP, Steel, BFRP, AFRP, and CFRP as well as fiber and non-fiber concrete were positioned within the GFRP profile in the tensile area during testing.

Throughout the experiments, the 400 mm span width was kept constant. The 500 mm long beam specimens were tested at a loading speed of 2 mm/min using a computer-connected flexural testing machine with a 50 kN capacity. There were displacements noted in the middle of the 400 mm span. Figure 2 illustrates the flexural testing of the specimens.

Table 1. Characteristics of FRP materials

	GFRP profile	Steel Bar	AFRP Bar	BFRP Bar	CFRP Bar	GFRP Bar
Specific gravity	1.78	7.68	1.42	1.55	1.55	1.87
Tensile Strength (MPa)	610	555	1320	1125	1340	950
Longitudinal rate (%)	41	–	74	74	74	74
Young Modulus (GPa)	31	200	60	55	125	48

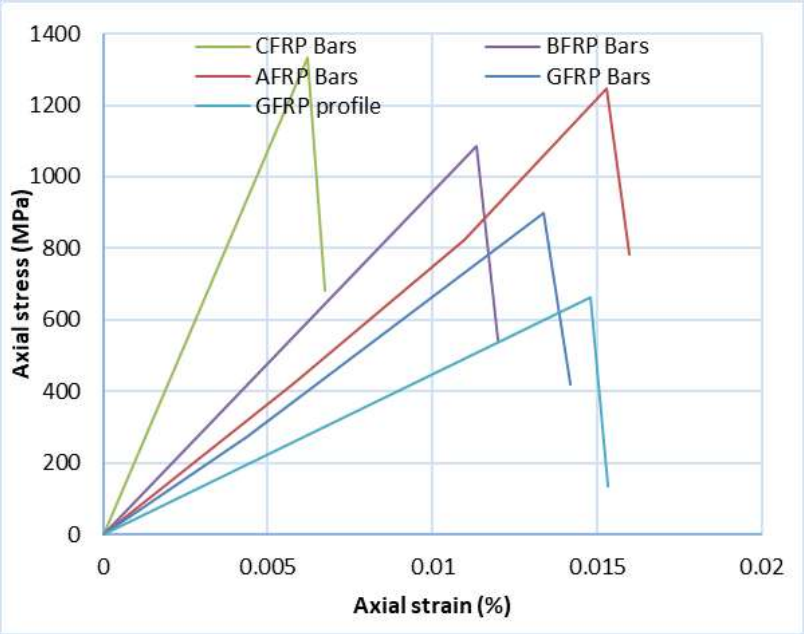

Figure 1. FRP bars and GFRP box profile tensile charts

Figure 2. Four-point beam tests

3. Tests and Results

3.1. Moment Curvature

To account for the structural response and non-linear features of different components, one needs to accurately analyze the moment curvature of different concrete sections. Henceforth, it is utmost important to assess different aspects which affect this parameter including geometric particulars and employed material. Henceforth, all the tested beams were evaluated for moment curvature by loading-displacement values derived by performing the three-point flexure testing. Later on, by taking the 2nd derivative of corresponding displacement parameter, the

curvature was obtained. Likewise, to obtain the desired parameter of moment curvature, following relationship can be referred (Eq. 1):

$$\frac{M_b(y)}{EI(y)} = \frac{d^2U_x}{dy^2} = \frac{1}{r(y)} \quad (1)$$

here Mb(y) designates the bending moment captured at any provide length, while E,I(y),U and r(y) explains the elastic moduli, moment of inertia, samples deflection in X-axis as well as the curvature radius.

3.2. Effect of Reinforcement Types

By utilizing the loading-displacement response from experimentation, the moment curvature plots were developed and compared. Figure 3a relates the moment curvature plots for concrete hybrid beam specimens without inclusion of the fibers. The moment capacity of the specimens developed by varying the bar types in plain concrete was found to be under 502.5 kN-mm, whereas the trend experienced an abrupt decline in associated capacity. However, those of the hybrid specimens (RH) having the plain concrete only developed the greatest value at 1648.2 kN-mm. The beam specimens strengthened by basalt fibers designated by RH-BFRP attained a lesser capacity compared to other counterparts and accomplished the greatest capacity of almost 2190.9 kN-mm. Likewise, the beam specimens strengthened by glass fiber bars of RH-GFRP attained the greatest capacity of almost 2311.5 kN-mm; however, the capacity response of RH-AFRP was as high as 2477.3 kN-mm. Also, the specimens having steel bars from the class of RH-Steel bar saw the moment capacity jump to the greatest outcome, being 2610.4 kN-mm. With the exception of plain concrete beams, all the hybrid specimens were found capable of sustaining the moment capacity even after breakage. Additionally, the specimens showed no signs of abrupt failure. For instance, Figure 3b illustrates the moment curvature plots of concrete with polypropylene fibers employed with GFRP box profiles. Though the hybrid beams of plain concrete experienced notable fractures, the specimens achieved a moment capacity of 1834.1 kN-mm, which was higher than those of the polypropylene fiber concrete (PFRC) beams, which had a comparatively lower capacity in flexure.

Nonetheless, the specimens from the class of PH-GFRP exhibited a capacity of 2420.4 kN-mm. The specimens also experienced a decline in stiffness value with an increase in flexure capacity. Compared to the CFRP strengthened beams, the specimens from the class of PH-AFRP and PH-CFRP exhibited respective capacities of 2562.8 kN-mm and 2691.4 kN-mm. However, the beams with CFRP reinforcement accomplished a comparatively greater capacity in flexure. Though PH-BFRP showed a few signs of fracture, the beams presented almost the same response as observed in the CFRP strengthened specimens, attaining a capacity value of almost 2324.7 kN-mm. Conversely, the PH-SFRP specimens with steel bars developed a capacity as high as 2480.4 kN-mm. Furthermore, the specimens designated by the class of PH-CFRP as well as PH-AFRP developed the greatest strength in flexure. Figure 3c illustrates the moment curvature plots for glass fiber-sourced hybrid beam specimens.

3.3. Effect of Concrete Strength

By employing the same bar types in hybrid specimens, the impact of varying fibers in concrete was evaluated on associated outcomes of the moment curvature. Figure 4a illustrates the variation in moment curvature for all the tested steel-strengthened beam specimens. PH-steel bar hybrid specimens as well as those of the RH-steel bar beams without fibers achieved almost similar capacities, reaching approximately 2512.5 kN-mm. GH-steel bar sourced hybrid specimens developed a capacity value of 3100.5 kN-mm, whereas SH-steel bar specimens exhibited the highest moment capacity, reaching 2600.5 kN-mm. Among other competing beams, the specimens

containing steel fiber and glass fiber showed a notable increase in moment capacity, along with an increase in associated ductility. However, the inclusion of polypropylene fiber did not impart any significant impact on the ductility and moment capacity.

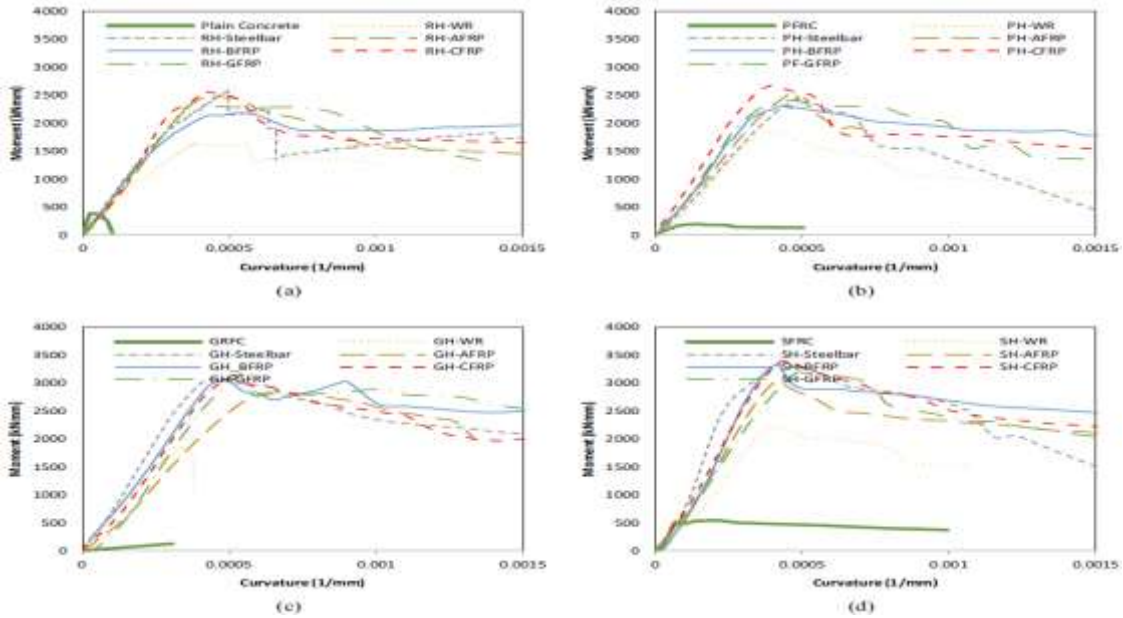

Figure 3. Moment-curvature plots of strengthened hybrid beam specimens a) non-fiber b) polypropylene fibers c) glass fibers d) steel fibers

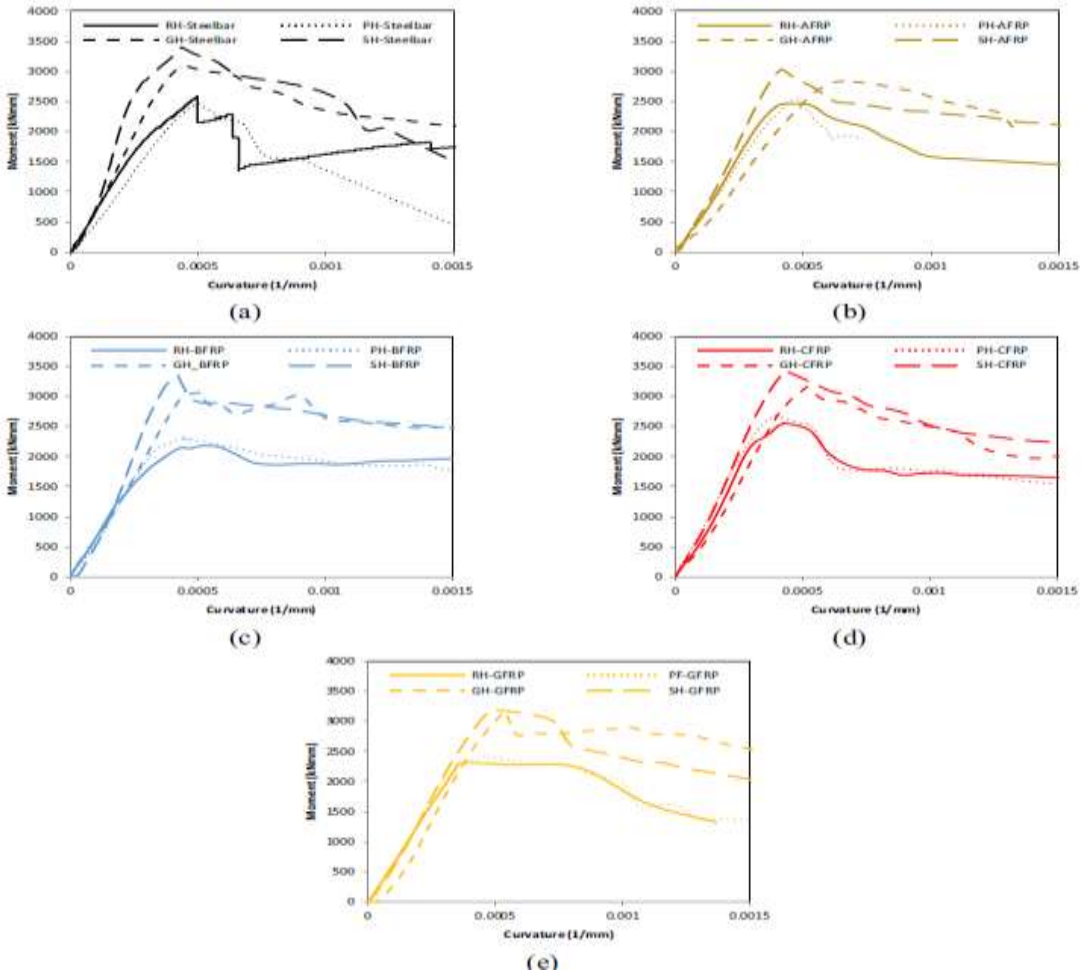

Figure 4. a) Moment-curvature plots of reinforced hybrid beam specimens a) steel bars b) AFRP bars c) BFRP bars d) CFRP bars e) GFRP bars

Figure 4b illustrates the variation in the moment-curvature response with fiber inclusion in the AFRP hybrid concrete beams. The RH-AFRP specimen without fibers developed a capacity of 2477.33 kN-mm, while the PH-AFRP specimens achieved a moment capacity of 2562.75 kN-mm. Similarly, the GH-AFRP and SH-AFRP beams sustained flexural loading and moment capacities of 2856.21 kN-mm and 3045.15 kN-mm, respectively. Regarding the two parameters of stiffness and moment capacity, the beams with steel fibers and glass fibers developed greater values than those of the specimens with polypropylene fibers and control beams, respectively. Figure 4c illustrates the fiber impact on the moment-curvature response of hybrid beams with BFRP. The moment capacities of the RH-BFRP and PH-BFRP were found to be 2190.9 kN-mm and 2324.57 kN-mm, respectively. Additionally, the PH-BFRP specimens presented a notable enhancement in stiffness after achieving a moment capacity of 2324.57 kN-mm.

In comparison, the greatest capacity of 3034.10 kN-mm for GH-BFRP specimens, the SH-BFRP beams developed the highest capacity value of 3356.7 kN-mm. The stiffness and flexural strength of the steel and glass fiber specimens were the highest among all the beams. Figure 4d illustrates the impact on the moment-curvature response of CFRP-strengthened beam specimens by varying the fibers. The RH-CFRP, PH-CFRP, GH-CFRP, and SH-CFRP specimens developed corresponding moment capacities of 2567.78 kN-mm, 2684.39 kN-mm, 3170.78 kN-mm, and 3417.00 kN-mm, respectively.

Among the beam specimens with steel fibers, the beams with glass fibers exhibited the greatest moment capacity. However, the beams with polypropylene fibers presented capacity values closer to those observed for beams without fibers. Figure 4e illustrates the variation in the moment-curvature response of GFRP-strengthened beam specimens. The RH-GFRP, PH-GFRP, GH-GFRP, and SH-GFRP specimens developed corresponding moment capacities of 2311.50 kN-mm, 2420.04 kN-mm, 3178.82 kN-mm, and nearly 3216.00 kN-mm. Among the beam specimens, those with steel fibers, glass fibers, and without fibers exhibited the greatest moment capacity, respectively.

3.4. Ductility

Ductility defines the deformation capability of a structural component when subjected to tension stresses. The deformation should be polymer in nature, while the system should be able to sustain the external stresses without any breakage or cracking. Additionally, the term also accounts for the ability of a material to absorb certain amounts of energy. To assess the ductility parameter of tested specimens, curvature outcomes from the moment curvature plots were referred to.

Figure 5a presents the variation in ductility with different bar types. For instance, steel-strengthened beams without fiber inclusion in hybrid specimens exhibited the greatest ductility outcome. Additionally, the ductility of steel-strengthened beam specimens was 175.5% more than those of the unreinforced beam specimens having steel fibers. Likewise, CFRP and GFRP strengthened beams presented 163.5% more ductility, while specimens reinforced with AFRP and BFRP were 50.5% and 125.5% more ductile, respectively.

When comparing the ductility of steel-reinforced specimens with those of the hybrid specimens having steel fibers, the analysis revealed that the steel-strengthened beams exhibited a highly ductile response. Additionally, the ductility of steel-strengthened beams was 134.5% greater than that of the unreinforced hybrid specimens.

Likewise, GFRP and BFRP strengthened beams presented 27.5% and 15.5% more ductility, while specimens reinforced with AFRP and CFRP were 37.5%

and 29.5% more ductile, respectively. When comparing the ductility of hybrid specimens having polypropylene fibers with those of the specimens having BFRP, the analysis revealed that the BFRP-strengthened beams exhibited a highly ductile response.

Additionally, the ductility of BFRP-strengthened beams was 256.5% greater than that of the unreinforced beams. Likewise, GFRP and steel-strengthened beams presented 137.5% and 184.5% more ductility, while specimens reinforced with AFRP and CFRP were 40.5% and 155.5% more ductile, respectively.

While comparing the ductility of steel-strengthened specimens with those of the hybrid specimens having glass fibers, the results portrayed that the steel-strengthened beams presented a highly ductile response.

Additionally, the ductility of steel-strengthened beams was 188.5% greater than that of the unreinforced beams. Likewise, GFRP and CFRP-strengthened beams presented 125.5% and 107.5% more ductility, while specimens reinforced with AFRP and CFRP were 35.5% and 59.5% more ductile, respectively.

Figure 5b reports the variation in ductility by varying the fiber types. For instance, specimens having steel fibers accomplished a highly ductile response compared to those of the specimens having no reinforcement.

In comparison with specimens having no fibers, the specimens with steel fibers showed 244.5% more ductility. Likewise, the beams having polypropylene fibers and those of the glass fibers accomplished 22.5% and 67.5% more ductility, respectively.

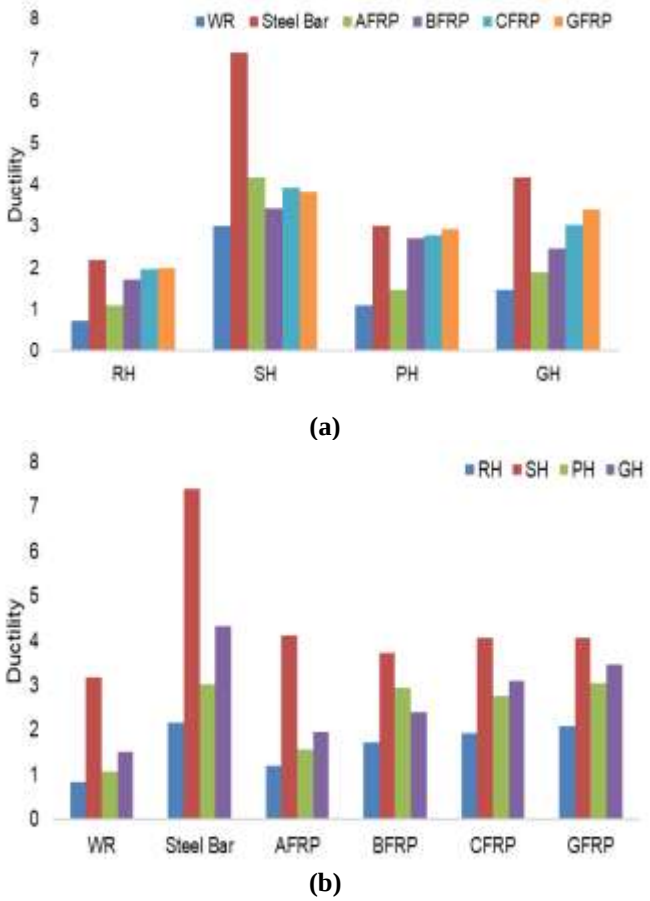

Figure 5. Comparison of ductility of hybrid beams a) by type of bar b) by type of fiber concrete

Mostly, the specimens having steel fibers with no reinforcement showed a highly ductile response by reporting 500.5% more ductility than those of the beams with no fibers. Likewise, the beams having polypropylene fibers and those of the glass fibers accomplished 42.5% and 96.5% more ductility, respectively. Additionally, the AFRP-strengthened specimens presented greater ductility for beams having steel fibers. This response was almost the same for those beams having steel reinforcement as well as the specimens with no reinforcement. Likewise, under the AFRP-strengthened class of specimens, the beams with steel fibers presented 254.5% more ductility than those beams having no reinforcement. Also, the beams having polypropylene fibers and those of the glass fibers accomplished 28.5% and 68.5% more ductility, respectively. Mostly, the specimens having polypropylene fibers under the class of BFRP-strengthened beams presented the greatest ductility by

showing 118.5% more ductility than those of the beams having no fibers. This response was also greater for the beams having steel fibers as well as those of the specimens with glass fibers. For instance, the specimens comprising steel fibers showed 98.5% more ductility, whereas the ductility response for the beams containing glass fibers was 32.5% more. Mostly, the specimens having steel fibers under the class of CFRP-strengthened beams presented the greatest ductility by showing 100.5% more ductility than those of the beams having no fibers. Also, the specimens comprising glass fibers showed 58.5% more ductility, whereas the ductility response for the beams containing polypropylene fibers was 40.5% more. Similarly, the specimens having steel fibers under the class of GFRP-strengthened beams presented the greatest ductility by showing 97.5% more ductility than those of the beams having no fibers. Additionally, the specimens comprising glass fibers showed 69.5% more ductility, whereas the ductility response for the beams containing polypropylene fibers was 50.5% more.

4. Conclusion

Following are the main findings of the present study:

- When comparing with bars types having WR, the Steel-bars and CFRP strengthened beams of RH class exhibited a 157.5% and 154.5% increase in moment capacity, respectively. Likewise, CFRP strengthened beams of SH class and PH class presented a 147.5% and 170.5% respective gain in moment capacity. Among these, the GFRP hybrid specimens with GH class accomplished the highest moment capacity.
- When comparing the fibers of RH class, the Steel-bars strengthened beams of SH class developed a 132.5% enhancement in flexure strength. Similarly, AFRP, BFRP, CFRP, and GFRP bars strengthened beams of SH class presented 123.5%, 153.5%, 133.5%, and 139.5% improvements in moment capacity, respectively. Among these, the GFRP hybrid specimens with SH class achieved the highest moment capacity.
- When comparing with bars types having WR, the Steel-bars strengthened beams of RH and SH class exhibited a 175.5% and 134.5% increase in ductility, respectively. Similarly, BFRP and Steel-bars strengthened beams of PH class and GH class presented a 273.5% and 188.5% respective gain in ductility. Among these, the GFRP hybrid specimens with GH class achieved the highest ductility.
- When comparing the fibers of RH class, the steel-bars strengthened beams of SH class developed a 244.5% enhancement in ductility. Similarly, SH-AFRP, SH-CFRP, SH-GFRP, and PH-BFRP strengthened beams presented 354.5%, 200.5%, 136.5%, and 167.5% improvements in ductility, respectively.

References

Ahmad, A. and A. Raza, Reliability analysis of strength models for CFRP-confined concrete cylinders. Composite Structures, 2020. **244**: p. 112312.

Aslam, H.M.U., A. Sami, and A. Raza, Axial compressive behavior of damaged steel and GFRP bars reinforced concrete columns retrofitted with CFRP laminates. Composite Structures, 2021. **258**: p. 113206.

Aslani, F., Y. Gunawardena, and A. Dehghani, Behaviour of concrete filled glass fibre-reinforced polymer tubes under static and flexural fatigue loading. Construction and Building Materials, 2019. **212**: p. 57-76.

Berradia, M., et al., Data-oriented analysis of axial capacity of externally CFRP-confined concrete columns transversely reinforced with steel hoops or spirals. Mechanics of Advanced Materials and Structures, 2022. **29**(27): p. 6543-6556.

Berradia, M., et al., Prediction of ultimate strain and strength of CFRP-wrapped normal and high-strength concrete compressive members using ANN approach. Mechanics of Advanced Materials and Structures, 2023: p. 1-23.

El Ouni, M.H. and A. Raza, Data-driven analysis of concrete-filled steel-tube CFRP-confined NSC columns. Mechanics of Advanced Materials and Structures, 2021: p. 1-22.

Hiremath, P.N. and S.C. Yaragal, Performance evaluation of reactive powder concrete with polypropylene fibers at elevated temperatures. Construction and Building Materials, 2018. **169**: p. 499-512.

Raza, A., B. Ali, and A.u. Rehman, Structural performance of steel-tube concrete columns confined with CFRPs: Numerical and theoretical study. Iranian Journal of Science and Technology, Transactions of Civil Engineering, 2021. **45**(3): p. 1575-1592.

Raza, A., B. Ali, and H.M.U. Aslam, Axial performance of hybrid fiber reinforced concrete columns having GFRP longitudinal bars and spirals. Journal of Building Engineering, 2021. **35**: p. 102017.

Raza, A., et al. Axial performance of GFRP composite bars and spirals in circular hollow concrete columns. in Structures. 2021. Elsevier.

Raza, A., et al. Performance evaluation of hybrid fiber reinforced low strength concrete cylinders confined with CFRP wraps. in Structures. 2021. Elsevier.

Raza, A., et al., Structural evaluation of recycled aggregate concrete circular columns having FRP rebars and synthetic fibers. Engineering Structures, 2022. **250**: p. 113392.

Raza, A., M.H. El Ouni, and J. Baili, Data-driven analysis on axial strength of GFRP-NSC columns based on practical artificial neural network tool. Composite Structures, 2022. **291**: p. 115598.

Raza, A., Q. Khan, and A. Ahmad, Reliability analysis of proposed capacity equation for predicting the behavior of steel-tube concrete columns confined with CFRP sheets. Computers and Concrete, 2020. **25**(5): p. 383-400.

Raza, A., Structural behavior of GFRP-reinforced circular HFRC columns under concentric and eccentric loading. Arabian Journal for Science and Engineering, 2021. **46**(5): p. 4239-4252.

Raza, A., T. Alomayri, and M. Berradia, Rapid repair of partially damaged GFRP-reinforced recycled aggregate concrete columns using FRP composites. Mechanics of Advanced Materials and Structures, 2021: p. 1-17.

Setvati, M.R. and Z. Mustaffa, Rehabilitation of notched circular hollow sectional steel beam using CFRP patch. Steel and Composite Structures, 2018. **26**(2): p. 151-161.